

Causes of supercapacitors ageing in organic electrolyte

Philippe Azaïs^a, Laurent Duclaux^a, Pierre Florian^b, Dominique Massiot^b,
Maria-Angeles Lillo-Rodenas^c, Angel Linares-Solano^c, Jean-Paul Peres^d,
Christophe Jehoulet^d, François Béguin^{a,*}

^a CRMD, CNRS-University, 1B rue de la Férellerie, 45071 Orléans Cedex 2, France

^b CRMHT, CNRS, 1D avenue de la Recherche Scientifique, 45071 Orléans Cedex 2, France

^c Department of Inorganic Chemistry, University of Alicante, Apartado de Correos 99, 03080 Alicante, Spain

^d SAFT, Direction de la Recherche, 111 Boulevard Daney, 33074 Bordeaux Cedex, France

Received 27 October 2006; received in revised form 3 June 2007; accepted 1 July 2007

Available online 7 July 2007

Abstract

In order to understand what causes supercapacitors ageing in an organic electrolyte (tetraethylammonium tetrafluoroborate – Et₄NBF₄ – 1 mol L⁻¹ in acetonitrile), the activated carbon electrodes were characterized before and after prolonged floating (4000–7000 h) at an imposed voltage of 2.5 V. After ageing, the positive and negative electrodes were extensively washed with pure acetonitrile in neutral atmosphere to eliminate the physisorbed species. Then, the carbon materials were dried and transferred without any contact with air to be studied by XPS, ¹⁹F NMR, ¹¹B NMR and ²³Na NMR. Decomposition products have been found in the electrodes after ageing. The amount of products depends on the kind of activated carbon and electrode polarity, which suggests redox reactions of the electrolyte with the active surface functionality. Nitrogen adsorption measurements at 77 K on the used electrodes showed a decrease of accessible porosity, due to trapping of the decomposition products in the pores. Hence, the evolution of the supercapacitor performance with time of operation, i.e. the capacity decrease and the resistance increase, are due to the decomposition of the organic electrolyte on the active surface of the carbon substrate, forming products which block a part of porosity. The concentration of surface groups and their nature were found to have an important influence on the performance fading of supercapacitors.

© 2007 Elsevier B.V. All rights reserved.

Keywords: Supercapacitors; Organic electrolyte; Activated carbon; Ageing; Electrolyte decomposition; Pores blocking

1. Introduction

Although supercapacitors are known since the early 1970s [1–3], they recently received a renewed interest [4]. Taking into account that the energy stored in capacitors is proportional to the square of voltage, high energy density prototypes based on activated carbons and organic electrolytes, operating with a voltage window of 2.5 V, have been developed by several industrial companies [5–9]. Within the last years, a tremendous number of studies were dedicated to improve the performance of supercapacitors by developing new types of carbon materials: carbon nanotubes [10–14], carbon nanofibers [15], carbon aerogel [16,17], carbon xerogel [18] and glassy carbon [19]. However, because of their low cost (1 F = \$0.01)

and expected good cycleability, activated carbon-based supercapacitors remain the lonely practical candidates for industrial applications, especially for electric vehicles and power quality devices.

Nevertheless, after a prolonged operation, supercapacitors based on activated carbons and organic electrolytes may demonstrate capacity fading and resistance increase, together with macroscopic phenomena such as gas evolution, increase of the electrodes mass, local separation of the coating layer from the metallic collector. Since long life is mandatory for the envisioned applications of supercapacitors, a better knowledge of the ageing mechanisms is required, in order to define strategies allowing these drawbacks to be circumvented. Surface functionality and porosity of activated carbons [20] should be certainly optimised in order to improve the long-term electrochemical performance in organic medium.

Previous studies performed in SAFT laboratories have demonstrated that ageing of supercapacitors based on activated

* Corresponding author.

E-mail address: beguin@cnrs-orleans.fr (F. Béguin).

carbons is not noticeably affected by the porous texture [21]. An exhaustive review of patents rather suggests that the surface functionality and the impurities (water, metals and heteroatoms such as oxygen) contained in the activated carbon electrodes could be responsible of the electrochemical fading and of the macroscopic effects. The surface functional groups of activated carbon affect capacitance [22,23], whereas the amplitude of leakage current depends essentially on the acidic surface groups [24]. Few ppm of water in the organic electrolyte depress significantly the potential window, having an influence on the capacity fading [8]. Both adsorbed water and surface groups may be decomposed at a voltage higher than 2.5 V, which leads to gases production and fading of the electrochemical performance [25]. The evolved gases are expected to be blocked in the pores of separator and activated carbon, giving rise to a resistance increase [26]. The resistance increase and the electrodes damages could be also attributed to the presence of oxygen [27] and metal impurities [28]. Finally, a progressive transformation of the binder used for the realization of the electrodes coating could be also responsible of the capacitance decrease and resistance increase during operating the capacitors [29].

Though several reasons, mainly related with the nature of the electrolyte or the surface functionality of activated carbons, are given to interpret the performance fading of organic electrolyte-based supercapacitors, there is not a clear description of the chemical evolution of the electrodes and of the corresponding mechanisms. Therefore in this study, two activated carbons with different physico-chemical properties have been used for the realization of supercapacitors in organic medium. After a prolonged floating at 2.5 V, the aged electrodes have been analysed by X-ray photoelectron spectroscopy (XPS), nuclear magnetic resonance (NMR), and nitrogen adsorption. From the results obtained on these supercapacitor cells, we demonstrate clearly that the electrolyte is decomposed on the electrode materials (i.e. activated carbon), leading to changes of their chemical composition, and to the ageing phenomenon.

2. Experimental

The two activated carbons used for building the supercapacitors are named Maxsorb and OPTI. OPTI is a typical synthetic activated carbon prepared by steam activation of a phenolic resin char. Maxsorb is obtained after activation of a petroleum pitch carbon by KOH at 850 °C, according to references [30–32]. The oxygen content in the activated carbons outgassed 24 h at 200 °C ($P_{\text{limit}} = 2 \times 10^{-6}$ mbar) was measured by elemental analysis at the “Laboratoire Central d’Analyse du CNRS” (Verneuil, France). The concentration of oxygenated surface groups was determined by acid–base titration, according to the process described in references [33,34]. Thermogravimetric analysis (TGA) has been performed on a Setaram 1600 analyser in order to estimate the water proportion contained in the two activated carbons.

Electrodes were prepared by coating an aluminium foil with an aqueous suspension of the active material (activated carbon, 87 wt%) mixed together with a carboxymethylcellulose binder

(CMC, 4 wt%), a plasticizer (styrenebutyrene rubber (SBR), 4 wt%) and a percolator (carbon black, 5 wt%). SAFT 3500 F supercapacitor prototypes [35], with symmetric electrodes, were built with Maxsorb or OPTI using 1 mol L⁻¹ Et₄N⁺ BF₄⁻ in acetonitrile as electrolyte. The capacitor electrodes were aged by the application of a 2.5 V constant voltage during 4000 h and 7000 h for Maxsorb and OPTI, respectively. Every 250 h, impedance spectroscopy spectra were recorded in the frequency range from 65 kHz to 10 mHz at open circuit voltage with 10 mV amplitude, using a Solartron SI 1260 analyser (Schlumberger). Capacitance at a frequency of 10 mHz was estimated from the impedance spectrum using the formula $C = 2\pi/(0.01.Z'')$, where Z'' is the imaginary part of impedance. Self-discharge tests have been performed with a potentiostat/galvanostat (VMP Biologic, France) every 250 h.

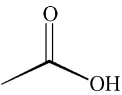
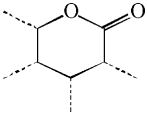
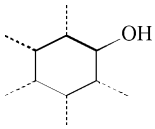
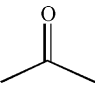
After applying 2.5 V permanent voltage, the capacitors were disassembled in a glove box, and the aged positive and negative electrodes were washed with acetonitrile during one week in a Kumagawa extractor under argon, in order to eliminate the physisorbed species. After washing, the electrodes were dried at 139 °C under vacuum during 1 week, and stored in a glove box. All the transfers have been performed under air-free atmosphere (vacuum or ultra pure argon) to avoid any modification of the aged electrodes by oxidation or hydration. For comparison purpose, fresh electrodes were washed and dried in the same conditions.

Nitrogen adsorption was measured at 77 K on the two activated carbons and on aged and fresh electrodes based on OPTI and Maxsorb, using an Autosorb 6 (Quantachrome). The OPTI and Maxsorb activated carbons were degassed at 200 °C for 15 h, whereas outgassing temperature of electrodes was only 140 °C in order to avoid any decomposition of the binder (CMC). The N₂ adsorption data were used to calculate the BET specific surface area S_{BET} .

The electrodes components (binder, plastifier, percolating agent and pure OPTI or Maxsorb), the fresh and aged electrodes were analysed by X-ray photoelectron spectroscopy (XPS) using an ESCALAB 250 (VG Scientific), after outgassing under secondary vacuum at 200 °C. The electrodes were progressively peeled under inert atmosphere, using an adhesive tape, allowing their composition to be determined by XPS as a function of depth, from the electrode/electrolyte interface to the aluminium foil.

In order to get more relevant information on all the active mass, Rotational Echo Double Resonance (REDOR) nuclear magnetic resonance (NMR) experiments have been performed on the powder from fresh and aged electrodes, using magic angle spinning (MAS) NMR on a DSX 400 (Bruker). This mode allows the volumetric 3D proximity of two elements to be determined on small amounts of disordered materials (X MAS: 12.5 kHz, $\nu_{\text{RF}} = 20$ kHz, use of T_{90} , recycle delays: 1 s; ¹⁹F MAS: use of Hahn Echo, 1 period, 12.5 kHz, $\nu_{\text{RF}} = 40$ kHz; REDOR: $\nu_{\text{R}} = 10$ kHz, $\nu_{\text{RF}}(\text{X}) = 20$ kHz, recycle delay: 1 s, evol.: 10 periods, $\nu_{\text{RF}}(^{19}\text{F}) = 40$ kHz). The selected references are 1 mol L⁻¹ NaCl in water for ²³Na NMR, the Et₂O → BF₃ complex for ¹¹B NMR and CClF₃ for ¹⁹F NMR. The powders were washed and dried according to the process described above. Rotor air-

Table 1
Concentration of surface groups (mequiv. g⁻¹) from the Boëhm [34] titration of OPTI and Maxsorb

					Bases
OPTI	0.04	0	0.88	0.1	0.33
Maxsorb	0.60	0	2.17	0	0.12

tight probes were filled in a glove box under ultra pure argon atmosphere.

3. Results and discussion

3.1. Physico-chemical and electrochemical characteristics of the activated carbons

Generally, activated carbons contain oxygenated surface groups, which type and concentration depend on the activation process [34]. From elemental analysis, the oxygen content is 1.7% and 6.2% for OPTI and Maxsorb, respectively. OPTI appears rather as a neutral carbon (pH in water 8.5) whereas Maxsorb is definitely acidic (pH in water 3.5). The results of acid–base titration on the two carbons show that the type and amount of oxygenated surface groups is very different (Table 1). The high concentration of acidic groups of Maxsorb well correlates with the oxygen content and macroscopic pH of this activated carbon. The important weight loss due to water evolution observed in the thermogram of Maxsorb below 200 °C (Fig. 1) confirms that the latter is more hydrophilic than OPTI, which fits well with its high concentration of acidic surface groups. This hydrophilic character of Maxsorb could be responsible of higher water retention in the electrodes fabricated from this material. Besides, coupling TGA with mass spectrometry analysis of the evolved gas, indicates that the further weight loss observed above 300 °C for Maxsorb is related with the elimina-

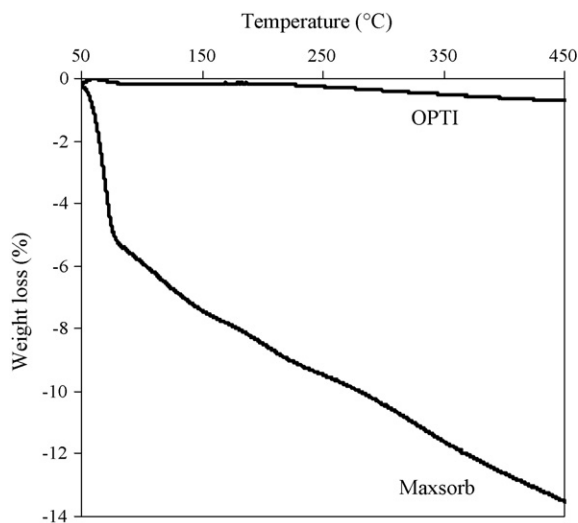


Fig. 1. Thermogravimetric analysis of Maxsorb and OPTI under argon atmosphere at a heating rate of 2 °C min⁻¹.

tion of CO₂, giving an additional confirmation for the presence of surface carboxylic groups in this carbon.

The nitrogen adsorption isotherms of Maxsorb and OPTI are both of type I, typical of essentially microporous materials. The pore size distribution is narrower for OPTI than for Maxsorb. The values of the BET specific surface area are close to 1600 m² g⁻¹ and 2500 m² g⁻¹, for OPTI and Maxsorb, respectively.

The electrochemical performance of capacitors built with OPTI and Maxsorb in 1 mol L⁻¹ Et₄N⁺ BF₄⁻ in acetonitrile has been monitored as a function of the floating time at 2.5 V. The values of the initial specific capacitance are 100 F g⁻¹ and 110 F g⁻¹ of OPTI and Maxsorb, respectively. As already claimed by several authors, these values are not directly correlated with the BET specific surface area, demonstrating that other parameters, such as the pore diameter, are also very important in the capacitance determination of a carbon material [36–38]. Fig. 2 shows that the capacitance of both materials decreases with the increase of floating time, and the fade is much higher for Maxsorb than OPTI. Simultaneously, the equivalent serial resistance (ESR) measured at 10 mHz increases with

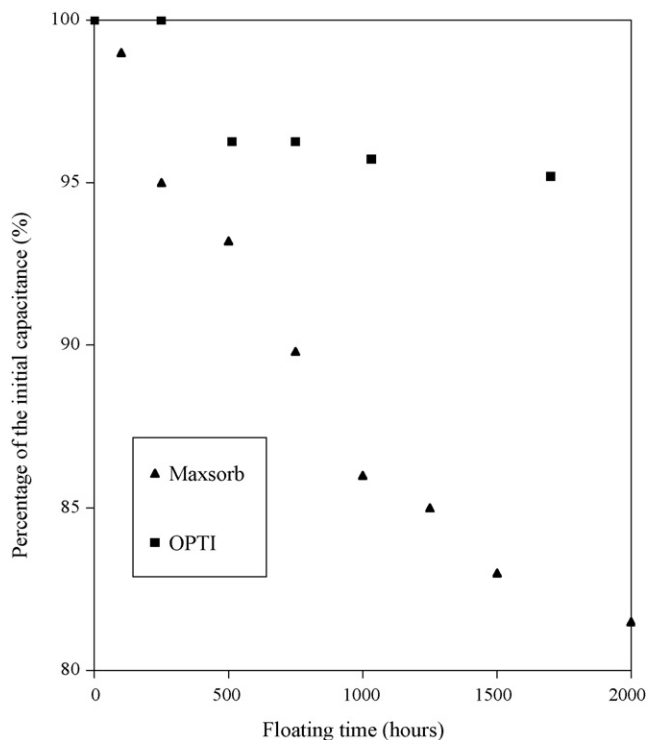


Fig. 2. Evolution of the capacitance of Maxsorb and OPTI with the floating time at 2.5 V.

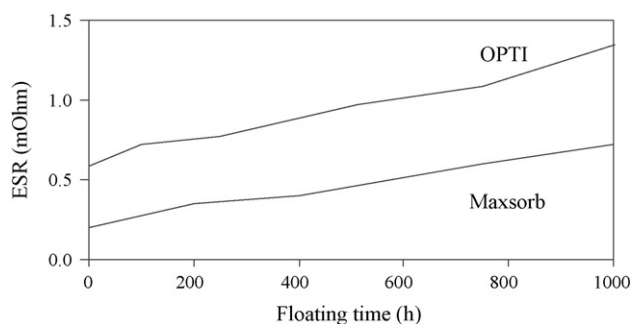


Fig. 3. Evolution of the ESR at 0.01 Hz of Maxsorb and OPTI with the floating time at 2.5 V.

increasing the time of permanent voltage application (Fig. 3). One must notice that the highest value of ESR is observed for the capacitor built with OPTI as electrode material. We believe that this difference of ESR between the two kinds of cells is essentially due to the conductivity of the electrode material itself. Indeed, the values of conductivity measured on the taped powders are 0.53 S cm^{-1} for Maxsorb and 0.23 S cm^{-1} for OPTI.

The open circuit voltage of capacitors based on OPTI and Maxsorb was measured after charging at 2.5 V during 30 min, in order to determine their self-discharge. For freshly built capacitors, the decrease of open circuit voltage after 70 h is lower for OPTI than Maxsorb (Fig. 4). This result fits well with a previous report showing that self-discharge depends on the amount of carboxylic groups [24]. By contrast, floating during 500 h prior measuring the evolution of open circuit voltage allows the self-discharge to be reduced, which is a confirmation of changes in the electrodes. A capacitor based on OPTI electrodes keeps well the charge after 500 h floating at 2.5 V.

3.2. Surface analysis of activated carbons and electrodes by XPS

XPS analyses indicate that pristine Maxsorb (Table 2) and OPTI (Table 3) powders contain quite small amount of oxygen (few percents). The fresh electrodes contain sodium and a high amount of oxygen, both elements being provided by the binder (carboxymethylcellulose). The elemental composition of positive and negative aged electrodes is qualitatively and quantitatively very different. The positive electrodes contain more nitrogen than the negative ones, especially on the surface, and

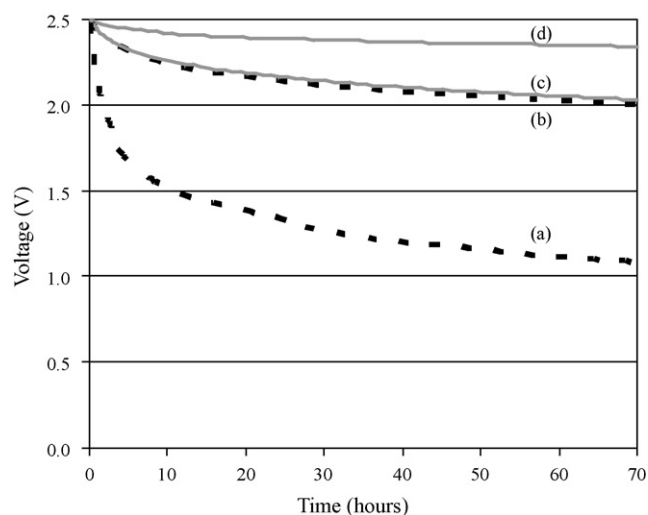


Fig. 4. Time dependence of the open circuit voltage for supercapacitors based on OPTI and Maxsorb. The capacitors were charged at 2.5 V during 30 min. (a, black dot-line) capacitor based on Maxsorb electrodes; (b, black dot-line) the same as (a) after 500 h floating at 2.5 V; (c, grey line) capacitor based on OPTI electrodes; (d, grey line) the same as (c) after 500 h floating at 2.5 V.

no sodium. The negative electrodes contain more fluorine than the positive ones, especially on the surface, and almost the same amount of sodium as in a raw electrode. One must note that, on the basis of Et_4N^+ and BF_4^- ions migration to the negative and positive polarities, respectively, just the opposite trend should be observed for the amount of nitrogen and fluorine in the two electrodes. On the other hand, the aged negative electrodes contain a very small amount of boron. This fact might suggest the decomposition of BF_4^- , as fluorine appears to be involved in different groups evidenced by XPS (the binding energies of 685.5 eV and 689 eV suggest NaF and CF groups). A negative concentration gradient was observed for Na, N, F from the electrolyte/electrode interface to the aluminium support, indicating that the electrolyte decomposition mainly takes place on the electrodes surface. By contrast, the decrease of the oxygen amount at the electrodes surface with ageing could be attributed to a partial dissolution of the binder in the electrolyte. Hence, capacitors from OPTI and Maxsorb seem to age by the same mechanism, probably due to similar electrochemical reactions involving electrolyte decomposition. Although the floating time was different for the two kinds of carbons, the surface chemistry of the electrodes after ageing is qualitatively similar.

Table 2

Atomic composition of Maxsorb based materials determined by XPS: as-received, fresh electrode, negative and positive electrodes aged by floating during 4000 h at 2.5 V

Element	As-received powder	Fresh electrode	Aged electrode (negative)		Aged electrode (positive)	
			Surface	Inside	Surface	Inside
B	0	0	0	0.3	0	0
Na	0	1.1	0.8	0.3	0	0
F	0	0	2.2	0.6	0.7	1
N	0	0	0.9	0	12.5	4
O	4	17.7	9.2	19.8	13.2	18.6

Analysis of the aged electrodes has been performed on the surface and after removing few layers.

Table 3
Atomic composition of OPTI-based materials determined by XPS: as-received, fresh electrode, negative and positive electrodes aged by floating during 7000 h at 2.5 V

Element	As-received powder	Fresh electrode	Aged electrode (negative)		Aged electrode (positive)	
			Surface	Inside	Surface	Inside
B	0	0	0.5	0.1	0	0.4
Na	0	1.6	1.7	0.4	0	0.3
F	0	0	5.6	0.6	0.8	0.9
N	0	0	1.5	1.1	16.6	1.5
O	5.4	22.0	19.3	21.3	13.8	23.6

Analysis of the aged electrodes has been performed on the surface and after removing few layers.

Electrolyte decomposition was also proved by gas evolution from the supercapacitor cells during floating. The main gases identified by gas chromatography were methane, ethane, di-oxygen, di-hydrogen, carbon monoxide and carbon dioxide. However, the emission of CO and CO₂ might be related with the binder decomposition.

3.3. Bulk NMR analysis

Contrary to XPS, magic angle spinning NMR allows all the volume of the aged carbon materials to be analysed. However, one must keep in mind that the sensitivity of the technique lies in particular on the natural abundance of the analysable isotope, being this fact an important drawback in some cases, as for example with carbon. Therefore, our experiments have been limited to three elements with 100% abundance, included either in the binder (sodium (²³Na)) or in the electrolyte (boron (¹¹B) and fluorine (¹⁹F)). The spatial proximity between two elements was detected by REDOR NMR [39–41]. Spatial proximity is detected when the elimination of the coupling signal between these two elements in each MAS NMR spectrum affects the respective peaks.

The electrolyte (1 mol L⁻¹ Et₄NBF₄ in acetonitrile) gives a single ¹⁹F NMR peak at -151.5 ppm versus CClF₃ and a single ¹¹B NMR peak at -1.1 ppm versus BF₃ in Et₂O. The fresh electrodes are free of fluorine and boron. On the other hand, the ²³Na MAS NMR spectra of fresh OPTI and Maxsorb electrodes present a single peak at 10.5 ppm versus 1 mol L⁻¹ NaCl in water, identical to that of the pure binder. The NMR results on aged Maxsorb and OPTI electrodes are summarised in Tables 4 and 5, respectively.

Table 4
NMR data on the aged Maxsorb electrodes

	¹¹ B NMR		¹⁹ F NMR		²³ Na NMR	
	Intensity (%)	δ (ppm), contribution (%)	Intensity (%)	δ (ppm), contribution (%)	Intensity (%)	δ (ppm), contribution (%)
Negative electrode	100	-1.3, 14% 7.2, 86%	100	-150.1, 11% -188.7, 89%	100	10.5, 62% 13.9, 33% 25, 5%
Positive electrode	77	-2.3, 27% 3.1, 73%	32	-156, 57% -199, 43%	43	16, 100%

The intensities are expressed in % of the most important contribution, i.e. the negative Maxsorb electrode.

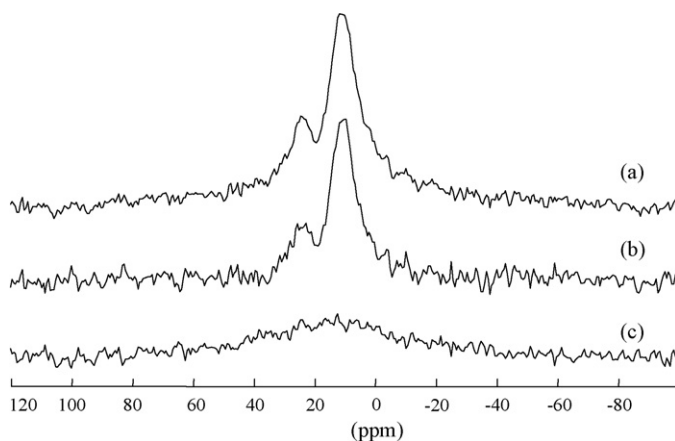


Fig. 5. Magic angle spinning NMR on the aged Maxsorb negative electrode. (a) ²³Na MAS NMR spectrum; (b) REDOR ²³Na-¹⁹F, i.e. (a) after removal of the coupling between Na and F; (c) difference (a) - (b).

3.3.1. NMR analysis of the aged Maxsorb electrodes (Table 4)

The ¹⁹F MAS NMR signal of the aged Maxsorb negative electrode is composed of two contributions. The amount of fluorine in this electrode (100%) is higher than in the positive one (32%) confirming the XPS analysis. The ²³Na MAS NMR spectrum shows three peaks, the contribution at 10.5 ppm being attributed to the original binder. The sodium content is higher in the negative electrode (100%) than in the positive one (43%) confirming also the XPS data. The difference between the ²³Na MAS NMR spectrum and the ²³Na REDOR MAS NMR spectrum of the aged Maxsorb negative electrode, obtained by annihilation of the coupling signal between fluorine and sodium, is presented in Fig. 5. The difference signal at ~10 ppm indicates a coupling

Table 5
NMR data on the aged OPTI electrodes

	¹¹ B NMR		¹⁹ F NMR		²³ Na NMR	
	Intensity (%)	δ (ppm), contribution (%)	Intensity (%)	δ (ppm), contribution (%)	Intensity (%)	δ (ppm), contribution (%)
Negative electrode	53	−1.2, 18% 7.5, 82%	–	–	96	10.5, 61% 10, 32% 25, 7%
Positive electrode	39	7.2, 100%	–	–	27	15.8, 100%

The intensities are expressed in % of the most important contribution, i.e. the negative Maxsorb electrode.

between a part of sodium and fluorine. It confirms the closeness of these two elements in the aged negative electrode. Nevertheless, the presence of NaF can be excluded, because it should give chemical shifts of 4 ppm and −126.7 ppm in ²³Na NMR and ¹⁹F NMR spectra, respectively.

The same method was applied to investigate the coupling between fluorine and boron. The ¹¹B MAS NMR signal shows two peaks at −1.3 ppm and 7.2 ppm, respectively. The signal/noise ratio of the difference obtained after tentative annihilation of the coupling between fluorine and boron is negligible, indicating that boron and fluorine atoms are separated.

According to these results, we can confirm that the electrolyte has been partly decomposed at the negative electrode, because of the appearance of new ¹⁹F NMR and ¹¹B NMR peaks and of the non-proximity of boron and fluorine detected by REDOR NMR experiments. Two new contributions have been also detected in the ²³Na NMR spectrum, demonstrating that sodium is involved in other chemical interactions, one possible being with fluorine.

Table 4 shows that the ¹⁹F MAS NMR signal of the aged Maxsorb positive electrode is composed of two distinct peaks, whereas the ²³Na MAS NMR spectrum contains a single line. This later contribution is quite broad compared with the pristine binder, suggesting a bulk modification of the binder in the aged positive electrode. However, the ²³Na REDOR MAS NMR with fluorine indicates non-proximity between fluorine and sodium, contrary to what is observed for the negative electrode. The signal/noise ratio of the difference signal using ¹¹B REDOR MAS NMR with fluorine is negligible. It leads to the conclusion that boron and fluorine are not close to each other and that the BF₄[−] anion from the electrolyte is decomposed. The presence of two peaks in the ¹⁹F NMR spectrum of the aged positive electrode compared to one peak in the pure electrolyte (Et₄NBF₄ in acetonitrile) leads to the same conclusion.

From the XPS and NMR data, it is unambiguously demonstrated that the chemical composition of the aged negative and positive electrodes from Maxsorb is different. Sodium has partly migrated from the positive to the negative electrode. Since the sodium species in the positive electrode are different from the original binder, this tends to demonstrate a change in the chemical environment of sodium. The boron concentration of the aged electrodes is quite small, and NMR shows that BF₄[−] is decomposed. All these facts tend to show that redox decomposition reactions of BF₄[−] take place on the surface of the Maxsorb electrodes, involving very likely the oxygenated surface groups.

3.3.2. NMR analysis of the aged OPTI electrodes (Table 5)

By contrast with the aged Maxsorb electrodes, fluorine was not detected by ¹⁹F MAS NMR on the aged OPTI electrodes, whatever their polarity.

The ²³Na MAS NMR spectra of the aged OPTI and Maxsorb electrodes are very similar. The ²³Na MAS NMR and XPS analyses of the aged OPTI electrodes fit well together, showing that sodium is present in higher amount in the negative electrode (96%) than in the positive one (27%). This general fact demonstrates that the essential contribution in the case of sodium is a migration of ions from the positive electrode to the negative one. The lower extent of self-discharge of the capacitors observed after floating is probably related with the trapping of sodium cations in the negative electrode.

The ¹¹B MAS NMR spectra of the aged OPTI and Maxsorb negative electrodes are also very similar, showing two peaks. According to these results, whatever the activated carbon, we can propose a similar redox decomposition mechanism of BF₄[−] on the negative electrode. For the aged OPTI positive electrode, the chemical shift of the ¹¹B NMR signal (7.2 ppm) also indicates that the BF₄[−] anion is decomposed.

3.4. Comparison of the aged OPTI and Maxsorb electrodes

Although the floating time was higher in the OPTI than in the Maxsorb-based supercapacitor (7000 h and 4000 h for OPTI and Maxsorb, respectively), the amount of boron was found to be about twice less in OPTI than in Maxsorb. Moreover, for the aged OPTI electrodes, fluorine was found to be present below the detection limit of ¹⁹F NMR, whereas it was detected by XPS. This discrepancy can be explained by the fact that XPS is a local analysis (beam size: 250 μm; depth < 10 nm) by contrast with NMR which probes the bulk of the materials. Hence, F observed by XPS in aged OPTI electrodes is locally grafted on some regions of heterogeneous surface, possibly on binder or plasticizer. Taking into account that the cycle life of OPTI supercapacitors is better than with Maxsorb, the NMR results tend to confirm that the electrolyte is less decomposed on OPTI than on Maxsorb. We can suggest that BF₄[−] anions are more efficiently decomposed in presence of Maxsorb due to the higher amount of oxygenated surface groups (Table 1) and/or adsorbed water in this activated carbon. However, it is very difficult to attribute the ¹¹B NMR chemical shift to a specific species because numerous boron containing chemicals may present a shift at around 7 ppm [42]. Among the possible species, tetravalent BF_xO_y[−] anions have a chemical shift in this region. The suggested BF_xO_y[−] ions

could be formed through BF_4^- decomposition in presence of water and/or oxygenated surface groups.

OPTI also differs from Maxsorb by a narrower pore size which may hinder the diffusion of solvated ions in OPTI. Mainly non-solvated ions can reach the active surface of OPTI [36,37,43] on which they are probably more stable than solvated ions. For Maxsorb, the active surface is more easily reached by the solvated ions. Due to the unavoidable presence of moisture during the preparation of the supercapacitor device, water molecules are also present in the pores of Maxsorb, where they enhance the dissociation of the carboxylic surface groups. In these conditions, the ions could undergo a “catalytic” decomposition due the acidic character of Maxsorb. A part of the observed fluorine species observed on the aged Maxsorb carbon could be grafted on the surface through C–F bonds. The oxygenated surface groups present on the carbon surface could favour such a fluorination reaction.

3.5. Nitrogen adsorption on fresh and aged electrodes

The objective of these measurements was to determine the influence of ageing on the porous texture of the electrodes. The fresh and aged electrodes were washed and dried using the conditions previously described in Section 2. By comparison with the raw activated carbon powder, the nitrogen adsorption measurements performed on the fresh electrodes reveal a small decrease of the BET surface area (Table 6), which is attributed to the blockage of some pores by the binder and/or the plasticizer. Nevertheless, all isotherms are still of type I (typical of microporous materials). After ageing, the specific surface area noticeably decreased for all the electrodes (Table 6). This result confirms that the products formed through the electrolyte decomposition on the electrodes block some micropores. However, at the ambient conditions of the floating experiments, this blockage cannot be attributed to some trapping of the gases previously identified by chromatography. Indeed, room temperature is extremely high compared to the temperatures allowing a noticeable adsorption of these gases in the micropores of carbon. The relative decrease of the BET specific surface area is more marked for the electrodes based on Maxsorb, whatever their polarity. Taking into account that the electrical double layer capacitance depends on the surface area of the electrode/electrolyte interface, this fact is directly related with the higher capacitance loss demonstrated by Maxsorb during floating (Fig. 2). The acidic surface groups present in larger amount in the case of Maxsorb might play a very significant role in the formation of decomposition products. Moreover, for both carbons, the decrease of specific surface area (Table 6), and consequently the amount of solid products formed by the redox decomposition of the electrolyte, is more important for the positive electrode than the negative one. Farahmendi et al. [8] have demonstrated that the potential window of the electrolyte is reduced by the presence of moisture, the effect being more pronounced for the positive range of potential than for the negative one. Hence, trace amounts of water in the electrolyte might play a significant role in the extent of the redox reactions which occur on both electrodes.

Table 6

BET specific surface area ($\text{m}^2 \text{g}^{-1}$) of OPTI and Maxsorb and of the fresh and aged electrode materials

	Maxsorb ($\text{m}^2 \text{g}^{-1}$)	OPTI ($\text{m}^2 \text{g}^{-1}$)
Powder	2500	1600
Fresh electrode	2350	1400
Aged negative electrode	1650	1130
Aged positive electrode	1280	980

Other parameters, such as the decrease of electrolyte concentration related with its decomposition, might have also some impact on the capacitance and on the electrolyte conductivity [44,45]. Additionally, the increase of serial resistance during floating (Fig. 3) can be interpreted by the formation of insulating products in the pores and/or the hindrance of ions diffusion.

4. Conclusion

Results presented here on SAFT 3500 F devices show that the ageing of supercapacitors is tightly related with the decomposition of the organic electrolyte on the active surface of carbon. The capacitance fading and serial resistance increase observed during the floating are directly related with the blockage of pores by decomposition products. Since the surface functionality and pore blocking are different for both electrodes, and since the electrolyte decomposition does not occur when electrodes are simply dipped in the solution without applying a polarization, this suggests that redox processes are responsible for ageing of supercapacitors. A poor surface functionality of carbon, enough narrow micropores and absence of moisture seem to be important requirements for a good life cycle of supercapacitors. On the other hand, we attribute the diminishing of self-discharge after floating to the trapping of the sodium ions, released by the binder, on the negative electrode.

References

- [1] D.I. Boos, US Patent 3,536,963 (1970), to Standard Oil Co.
- [2] B.E. Hart, R. M. Peekema, US Patent 3,652,902 (1972), to IBM.
- [3] V.P. Zykov, A.A. Panov, P.A. Prudnikov, M.I. Khlopina, A.D. Shlyapnikov, US Patent 3,675,087 (1972).
- [4] R. Kötze, M. Carlen, *Electrochim. Acta* 45 (2000) 2483–2498.
- [5] T. Morimoto, K. Hiratsuka, Y. Sanada, H. Aruga, US Patent 4,725,927 (1988), to Asahi Glass Co. and Elna Co. Ltd.
- [6] J. Tabuchi, T. Saito, A. Ochi, Y. Shimizu, US Patent 5,172,307 (1992), to NEC Corp.
- [7] A. Yoshida, K. Imoto, US Patent 5,150,283 (1992), to Matsushita Electric Industrial Co. Ltd.
- [8] J.C. Farahmendi, J.M. Dispenette, E. Blank, A.C. Kolb, WO9815962 (1998), to Maxwell Technologies.
- [9] C. Wei, E.C. Jarabek, O.H. Leblanc JR, WO0019464 (2001), to General Electric Co.
- [10] E. Frackowiak, S. Delpeux, K. Jurewicz, K. Szostak, D. Cazorla-Amoros, F. Béguin, *Chem. Phys. Lett.* 361 (2002) 35–41.
- [11] C.Y. Liu, A.J. Bard, F. Wudl, I. Weitz, J.R. Heath, *Electrochem. Solid State Lett.* 2 (1999) 577–578.
- [12] Ch. Emmenegger, P. Mauron, A. Züttel, Ch. Nützenadel, A. Schneuwly, R. Gallay, L. Schlapbach, *Appl. Surf. Sci.* 162–163 (2000) 452–456.
- [13] R.Z. Ma, J. Liang, B.Q. Wie, B. Zhang, C.L. Xu, D.H. Wu, *J. Power Source* 84 (1999) 126–129.

- [14] B. Zhang, J. Liang, C.L. Xu, B.Q. Wei, D.B. Ruan, D.H. Wu, *Mater. Lett.* 51 (2001) 539–542.
- [15] P.V. Adhyapak, T. Maddanimath, S. Pethkar, A.J. Chandwadkar, Y.S. Negi, K. Vijayamohanam, *J. Power Source* 109 (2002) 105–110.
- [16] J.L. Kaschmitter, S.T. Mayer, R.W. Pekala, US Patent 5,789,338 (1998), to Regents of the University of California.
- [17] R.W. Pekala, J.C. Farmer, C.T. Alviso, T.D. Tran, S.T. Mayer, J.M. Miller, B. Dunn, *J. Non-Cryst. Solids* 225 (1998) 74–80.
- [18] H. Pröbstle, C. Schmitt, J. Fricke, *J. Power Source* 105 (2002) 189–194.
- [19] M.G. Sullivan, R. Kötzt, O. Haas, *J. Electrochem. Soc.* 147 (2000) 308–317.
- [20] L.R. Radovic, C. Moreno, J. Rivera-Utrilla, in: L.R. Radovic (Ed.), *Chemistry and Physics of Carbon 27*, Marcel Dekker, Basel and New York, 2001.
- [21] L. Moreau, Ph.D. Thesis, University Pierre and Marie Curie (Paris VI), 2000.
- [22] T. Morimoto, K. Hiratsuka, Y. Sanada, K. Kurihara, *J. Power Source* 60 (1996) 239–247.
- [23] W. Qiao, Y. Korai, I. Mochida, Y. Hori, T. Maeda, *Carbon* 40 (2002) 351–358.
- [24] A. Yoshida, I. Tanahashi, A. Nishino, *Carbon* 28 (1990) 611–615.
- [25] M. Takeuchi, K. Koike, A. Mogami, T. Maruyama, US Patent 0,039,275 (2002), to JEOL Ltd.
- [26] E.C. Jerabek, S.F. Mansfield, US Patent 6,084,766 (2000), to General Electric Co.
- [27] J. Day, A.P. Sharipo, E.C. Jerabek, US Patent 6,110,321 (2000), to General Electric Co.
- [28] N. Sugo, H. Iwasaki, G. Uehara, European Patent EP 1176617 (2002), to Kuraray.
- [29] K. Nakao, K. Shimizu, T. Yamaguchi, US Patent 6,246,568 (2001), to Matsushita Electric Industrial Co. Ltd.
- [30] H. Marsh, D. Crawford, T.M. O’Grady, A.N. Wennerberg, *Carbon* 20 (1982) 419–426.
- [31] A.N. Wennerberg, US Patent 3,624,004 (1971), to Standard Oil Company.
- [32] A.N. Wennerberg, R.M. Alm, French Patent FR 2002047 (1969), to Standard Oil Company.
- [33] R.C. Bansal, D.B. Donnet, H.F. Stoekli, *Active Carbon*, Marcel Dekker, Inc., New York and Basel, 1988.
- [34] H.P. Boehm, *Adv. Catal.* 16 (1966) 179–274.
- [35] V. Danel, J.P. Flipo, X. Andrieu, B. Pichon, S. Barusseau, US Patent 6,356,432 (1997), to Alcatel Alsthom Compagnie Générale d’Electricité.
- [36] E. Raymundo-Pinero, K. Kierzek, J. Machnikowski, F. Béguin, *Carbon* 44 (2006) 2498–2507.
- [37] J. Chmiola, G. Yushin, Y. Gogotsi, C. Portet, P. Simon, P.L. Taberna, *Science* 313 (2006) 1760–1763.
- [38] J. Leis, M. Arulepp, A. Kuura, M. Lätt, E. Lust, *Carbon* 44 (2006) 2122–2129.
- [39] C.P. Grey, A.J. Vega, *J. Am. Chem. Soc.* 117 (1995) 8232–8242.
- [40] T. Gullion, J. Schaeffer, *Adv. Magn. Reson.* 13 (1989) 57–83.
- [41] T. Gullion, J. Schaeffer, *J. Magn. Reson.* 81 (1989) 196–200.
- [42] R.R. Gupta, M. Jain, P. Pardasani, R.T. Parsadani, A. Pelter, in: R.R. Gupta, M.D. Lechner (Eds.), *Nuclear Magnetic Resonance Data*, vol. 35. Group III: Condensed Matter, Springer-Verlag, Berlin, Heidelberg, New York, 1997.
- [43] C. Vix-Guterl, E. Frackowiak, K. Jurewicz, M. Friebe, J. Parmentier, F. Béguin, *Carbon* 43 (2005) 1293–1302.
- [44] M. Ue, K. Ida, S. Mori, *J. Electrochem. Soc.* 141 (1994) 2989–2996.
- [45] J.P. Zheng, T.R. Jow, *J. Electrochem. Soc.* 144 (1997) 2417–2420.